

Receiver Design for an Optical MIMO Testbed

Heidi Köhnke, Robert Schwinkendorf, Sebastian Daase, Andreas Ahrens and Steffen Lochmann
Hochschule Wismar, University of Technology, Business and Design, Philipp-Müller-Straße 14, 23966 Wismar, Germany

Keywords: Multiple-input Multiple-output System, Optical Fibre Transmission, Multimode Fiber (MMF), Mode Coupling.

Abstract: Within the last years multiple-input multiple-output (MIMO) systems have attracted a lot of attention in the optical fibre community. Although the theoretical background of MIMO transmission is well understood, there is still a need for practical investigations regarding mode combining, mode maintenance and mode splitting. Since these components represent an essential part of an optical MIMO system, in this work a (2×2) MIMO testbed using fusion couplers and a multi-mode fibre (MMF) length of 1.9 km is set up for an operating wavelength of 1326 nm. Together with the MIMO receiver-side signal processing the successful transmission of parallel data streams is presented.

1 INTRODUCTION

The growing demand of bandwidth particularly driven by the developing Internet has been satisfied so far by optical fibre technologies such as Dense Wavelength Division Multiplexing (DWDM), Polarization Multiplexing (PM) and multi-level modulation. These technologies have now reached a state of maturity (Winzer, 2012). The only way to further increase the available data rate is now seen in the area of spatial multiplexing (Richardson et al., 2013), which is well-established in wireless communications (Tse and Viswanath, 2005; Kühn, 2006). Nowadays several novel techniques such as Mode Group Diversity Multiplexing (MGDM) (Franz and Blow, 2012) or Multiple-Input Multiple-Output (MIMO) are in the focus of interest (Singer et al., 2008).

Among these techniques, optical MIMO has shown its capability for high-speed data transmission. However, the practical implementation has to cope with many technological obstacles such as mode multiplexing and management. This includes mode combining, mode maintenance and mode splitting.

In order to investigate these effects in a whole transmission system a MIMO testbed has been set up. Here, fusion couplers are used for mode combining and splitting realizing a parallel data transmission over a 1.9 km multi-mode fibre (MMF) (Ahrens and Lochmann, 2013; Sandmann et al., 2014a; Sandmann et al., 2014b). For the necessary implementation of the MIMO signal processing an off-line MIMO re-

ceiver has been programmed.

Against this background the novelty of this paper is the practical receiver implementation within a (2×2) MIMO testbed using fusion couplers. Its proper mode of operation is shown by the eye diagram.

The remaining part of the paper is structured as follows: In section 2 the optical MIMO testbed and its corresponding system model are introduced. The further processing of the measured data, which is carried out by off-line signal processing, is described in section 3. Section 4 presents the investigated equalizer design. The obtained results are given in section 5. Finally, section 6 shows our concluding remarks.

2 OPTICAL MIMO SYSTEM MODEL

The principle of optical MIMO is based on the activation of different modes or mode groups respectively, as illustrated in Fig. 1. In order to realize a parallel data transmission different data sources make use of these mode groups. A possible solution is the excitation of low order mode (LOM) and high order mode (HOM) groups. These different modes travel together in a MMF and can be separated by their spatial distribution at the receiver side leading to a (2×2) MIMO system in this contribution.

The excitation of the different modes can be done through various methods. Besides using Spatial Light Modulators (SLM) (Gu et al., 2013), Long-Period

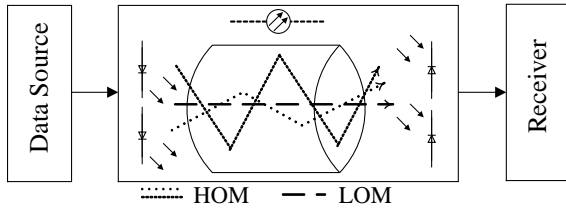


Figure 1: Optical MIMO system by activating LOM and HOM groups.

Gratings (LPG) (Giles et al., 2012) or Photonic Crystals (Amphawan and Al Samman, 2013), the excitation can simply be carried out by a centric or an eccentric splice between a single-mode fibre (SMF) and a MMF. Fig. 2 illustrates a typical eccentric splice used to excite HOM groups. Unfortunately, two SMFs' can't easily be placed in front of standard MMF. That's why other solutions are in the focus of interest. Investigations in (Ahrens and Lochmann, 2013) have shown that fusion couplers are capable of combining different mode groups into a MMF.

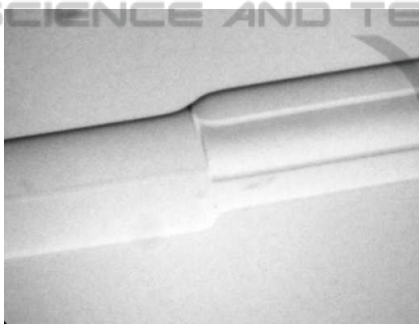


Figure 2: Eccentric single to multi-mode fibre splice (eccentricity $20 \mu\text{m}$).

For mode separation at the receiver side fusion couplers similar to the transmitter side are used. The structure of the corresponding practical testbed is shown in Fig. 3.

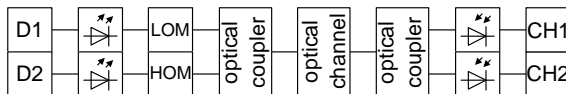


Figure 3: Structure of the optical (2×2) MIMO testbed.

Two independent data sources (D1, D2) realized by an Agilent high-speed pattern generator N4903B produce unipolar signals, which drive the respective laser diode modules with a pulse frequency of $f_T = 625 \text{ Mbit/s}$. The laser diodes can either work at 1326 nm or 1576 nm . Their light is fed to the centric and eccentric splice with different power. The laser diode, which has the higher power is used for activating the HOM, to compensate for the losses of higher

modes. Thereafter they are combined by the fusion coupler. After the fibre length of 1.9 km , the transmitted signals are separated by the second fusion coupler followed by two broadband Agilent 81495A receivers. The obtained signals are sampled by a high-speed sampling oscilloscope (Agilent DSO90804A) and stored for further off-line signal processing (CH1, CH2). Fig. 4 shows the corresponding electrical MIMO system model.

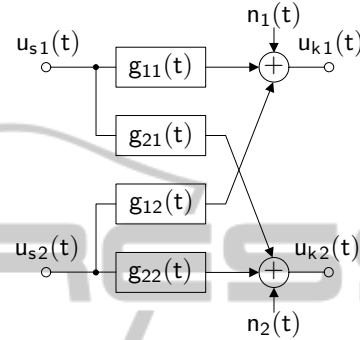


Figure 4: (2×2) MIMO system model.

The n_T transmit signals $u_{s\mu}(t)$ (for $\mu = 1, \dots, n_T$) are mapped to the n_R received signals $u_{kv}(t)$ (for $v = 1, \dots, n_R$) by using the corresponding impulse responses $g_{v\mu}(t)$. Additionally, white Gaussian noise $n_v(t)$ (for $v = 1, \dots, n_R$) is added at the receiver side. Mathematically, the received signals can be described as

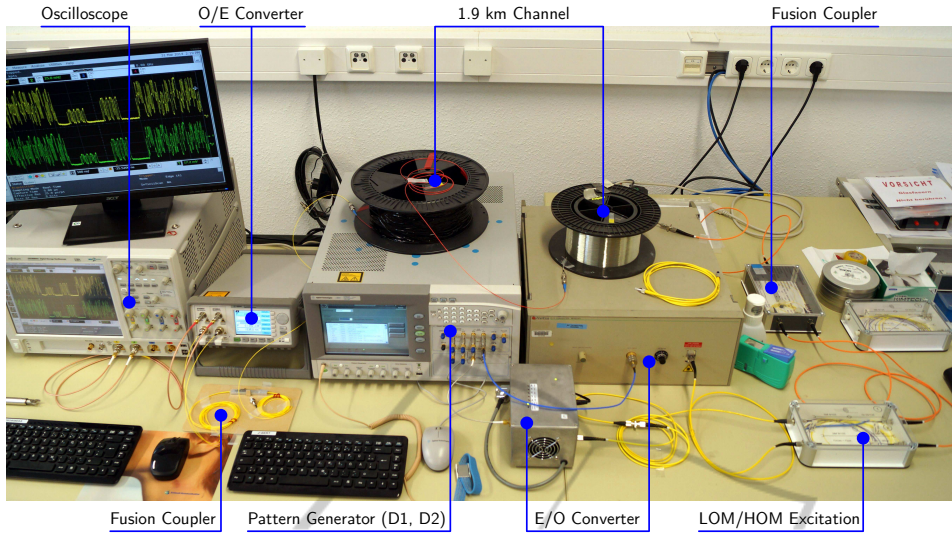
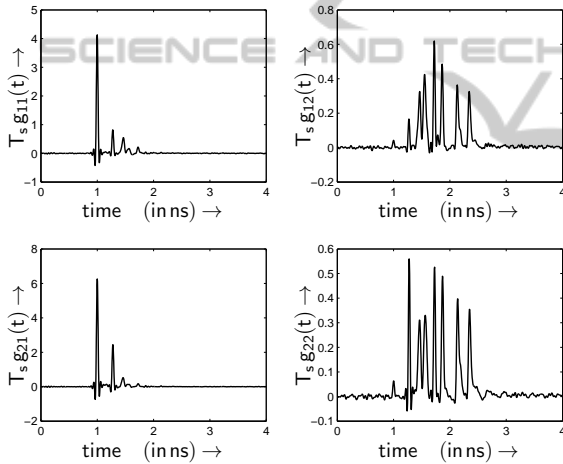
$$u_{kv}(t) = \sum_{\mu=1}^{n_T} u_{s\mu}(t) * g_{v\mu}(t) + n_v(t) . \quad (1)$$

In this paper the number of transmitters and receivers is limited to $n_T = n_R = 2$. The setup of the practical (2×2) MIMO system is shown Fig. 5.

Fig. 6 shows the measured impulse responses of all underlying channels of this (2×2) MIMO system (Ahrens and Lochmann, 2013). From Fig. 6 it can be seen by comparing the impulse responses $g_{11}(t)$ and $g_{22}(t)$ that the mode groups can be separated efficiently. Moreover, a typical high cross talk can be identified from $g_{12}(t)$ and $g_{21}(t)$.

3 OFF-LINE SIGNAL PROCESSING

In the following the off-line signal processing is described including symbol clock recovery, frame synchronisation, channel estimation and equalisation. Referring to Fig 4, the MIMO channel can be divided into four individual SISO channels. Fig. 7 shows such

Figure 5: Setup of the practical (2×2) MIMO system.Figure 6: Measured MIMO specific impulse responses applying a pulse frequency of $f_T = 1/T_s = 625$ Mbit/s (fibre length of 1.9 km and diode laser wavelength 1326 nm).

a SISO channel with its corresponding off-line processing components, which have to be combined in case of MIMO transmission.

The starting transmitter block includes a rectangular transmit filter $g_s(t)$. It is followed by the SISO channel described by its respective impulse response. The receiver consists of rectangular filter $g_{ef}(t)$ and the corresponding off-line signal processing components.

3.1 Symbol Clock Recovery

The method of the symbol clock recovery is highlighted in Fig. 8. The received signals $u_{kv}(t)$ of both MIMO-channels (i. e. for $v = 1, 2$) have to be squared

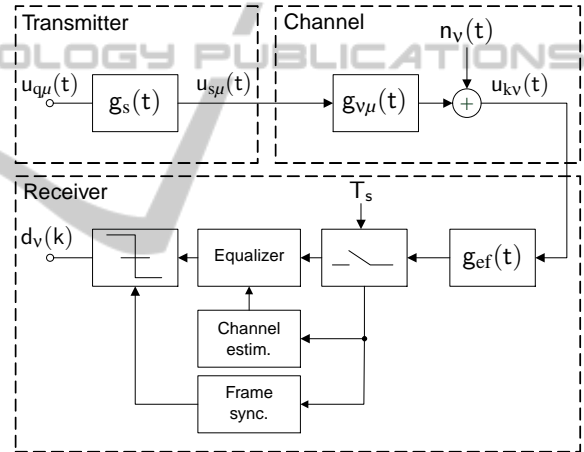


Figure 7: SISO system model.

in order to obtain a frequency component at the symbol pulse frequency. After bandpass filtering with the symbol frequency the symbol clock can be found and the sampled received signal $u_v(k)$ is obtained.

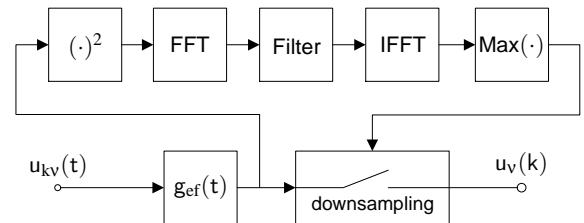


Figure 8: Symbol clock recovery.

3.2 Frame Synchronization and Channel Estimation

The sampled data are the input data for frame synchronization and channel estimation. The data structure of the transmitted signal is organized as follows: The payload data are packed into 1024-bit long frames. The structure of this frame is shown in Tab. 1. Each frame consists of 784 bit payload (R), a 52 bit training sequence (T) and 188 zeros (0) as guard interval to compensate the delay time difference. The 52 bit training sequence consists of two 26 bit long GSM training sequences. Since the paper concentrates on the prove of the optical MIMO concept, the length of the given sequences isn't in the focus of the testbed optimization.

The balanced 26 bit training sequence, which relates to GSM standard, is used for the synchronization and the training of the adaptive equalizer. To find the 52 bit sequence (T) in the data stream, the cross-correlation function between the training sequence and the data stream is calculated. The resulting cross-correlation peak is now used for the frame synchronisation. Furthermore, it is possible to estimate the channel coefficients by the cross-correlation function of the inner 16 bit of the 26 bit orthogonal GSM training sequence and the corresponding sequence of the measured data.

4 EQUALISER DESIGN

The equalization of the filtered and sampled receive signals $u_v(k)$ refers to the principle of van Etten (van Etten, 1975; van Etten, 1976), which is illustrated in Fig. 9. Using the channel impulse responses $h_{v\mu}(k)$, which describe the mapping of the μ th input to the v th output, i. e.

$$h_{v\mu}(t) = g_s(t) * g_{v\mu}(t) * g_{ef}(t) , \quad (2)$$

the whole MIMO system can be decomposed into a number of SISO channels. These SISO channels include the impact of the channel as well as the transmit and receive filtering. It is assumed that the $h_{v\mu}(k)$ of each SISO channel consist of $L + 1$ non-zero coefficients. Furthermore, the noise components $w_v(k)$ are obtained after receive filtering and sampling of $n_v(t)$.

In order to remove the MIMO interferences, i. e. interferences between the different input data streams as well as intersymbol interferences, an appropriate equalizer has to be chosen. A possible solution was introduced in (van Etten, 1975; van Etten, 1976) for estimating the corresponding MIMO specific equalizer coefficients $f_{v\mu}(k)$ (with $v = 1, 2$ and $\mu = 1, 2$).

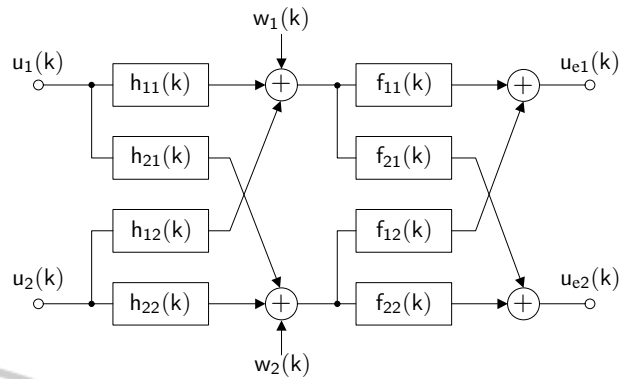


Figure 9: (2×2) MIMO equalizer.

The equalizer is determined similar to the zero forcing (ZF) T -spaced equalizer known from baseband or single-carrier transmission (Bingham, 1988).

In order to describe the whole MIMO system, (2×2) submatrices \mathbf{H}_ℓ (for $\ell = 0, \dots, L$) have to be created taking the impact of the (2×2) MIMO channel at the time ℓ into account, i. e. $h_{v\mu}[\ell]$. The (2×2) submatrices \mathbf{H}_ℓ result in

$$\mathbf{H}_\ell = \begin{bmatrix} h_{11}[\ell] & h_{12}[\ell] \\ h_{21}[\ell] & h_{22}[\ell] \end{bmatrix} . \quad (3)$$

Taking the $L + 1$ non-zero coefficients of the impulse responses $h_{v\mu}(k)$ into account, the interferences within the MIMO system are described by the channel convolution matrix \mathbf{H} , which is given by

$$\mathbf{H} = \begin{bmatrix} \mathbf{H}_0 & \mathbf{0} & \dots & \mathbf{0} \\ \mathbf{H}_1 & \mathbf{H}_0 & \dots & \mathbf{0} \\ \vdots & \vdots & \ddots & \vdots \\ \mathbf{H}_L & \mathbf{H}_{L-1} & \dots & \mathbf{H}_0 \\ \mathbf{0} & \mathbf{H}_L & \dots & \mathbf{H}_1 \\ \vdots & \vdots & \ddots & \vdots \\ \mathbf{0} & \mathbf{0} & \dots & \mathbf{H}_L \end{bmatrix} , \quad (4)$$

where $\mathbf{0}$ is a (2×2) zero matrix.

With the knowledge of the channel matrix \mathbf{H} a multidimensional equalizer can be derived similar to the T -spaced equalizer known from the baseband transmission. At first a 2-dimensional Nyquist vector

$$\mathbf{z} = (\mathbf{0} \dots \mathbf{0} \mathbf{I} \mathbf{0} \dots \mathbf{0}) \quad (5)$$

is defined, where $\mathbf{0}$ is a (2×2) zero matrix and \mathbf{I} denotes a (2×2) identity matrix. The equalizer is given according to

$$\mathbf{F} = (\mathbf{H}^T \cdot \mathbf{H})^{-1} \cdot \mathbf{H}^T \cdot \mathbf{z}^T \quad (6)$$

The position of the (2×2) identity matrix \mathbf{I} within the matrix \mathbf{z} is a degree of freedom to adapt the equalizer

Table 1: Frame structure consisting of training sequences (T), guard intervals (0) and data (R).

D1 (LOM)	T	T	0	0	0	0	0	0	R	0
D2 (HOM)	0	0	0	0	T	T	0	0	R	0
bit	26	26	26	26	26	26	26	26	784	32
	←				1024 bit				→	

to the channel conditions. Now the equalizer matrix \mathbf{F} can be rewritten as

$$\mathbf{F} = (\mathbf{e}_1^T \mathbf{e}_2^T) \quad (7)$$

and the decomposition of the μ th column \mathbf{e}_μ^T provides the equalizer impulse response $f_{v\mu}(k)$, which connect the μ th ($\mu = 1, 2$) receive filter output to the v th equalizer output ($v = 1, 2$). With the proposed ZF equalizer, the MIMO inherent interferences are removed at the cost of an increased noise power at the detector input.

5 RESULTS

In this contribution, the channel measurements are carried out within a 1.9 km (2×2) MIMO system. For this, the HOM groups were excited by an eccentricity of 15 μm . Fig. 10 and Fig. 11 illustrate the combination of each MIMO signal $u_{kv}(t)$ by superposition of the SISO channels $u_{kv\mu}(t)$.

Taking (1) into account, the MIMO signal at the output v (for $v = 1, 2$) is obtained as

$$u_{kv}(t) = u_{kv1}(t) + u_{kv2}(t) + n_v(t) . \quad (8)$$

Therein the received signals $u_{kv1}(t)$ and $u_{kv2}(t)$ describe the influence of the transmitter 1 and 2, respectively. Furthermore, there is a time delay between the respective transmitted training sequence and the crosstalk, caused by a different fiber length between source and coupler of each input, which has been compensated by the frame synchronisation module.

Based on the measured receive signals $u_{kv}(t)$ the channel coefficients $h_{v\mu}(k)$ can be estimated, which is shown in Fig. 12. With the estimated channel coefficients the time-dispersive nature of the underlying transmission channel is visible. After estimating the channel coefficients $h_{v\mu}(k)$, the multidimensional equalizer can be formed in order to remove the interferences from the MIMO system. The corresponding eye-diagram is shown in Fig. 13 for the equalized signal $u_{e1}(t)$.

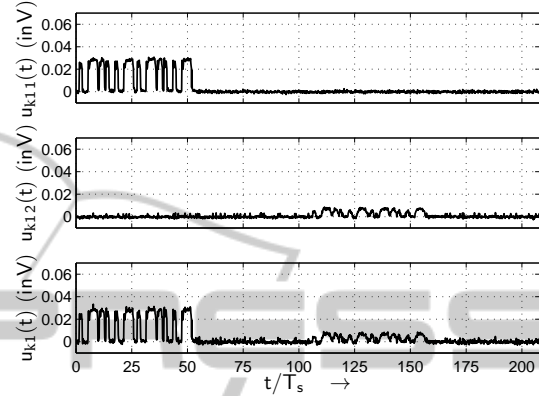


Figure 10: Measured received signal $u_{k1}(t)$ within the (2×2) MIMO system with respect to the pulse frequency $f_T = 1/T_s = 625$ assuming a fibre length 1.9 km.

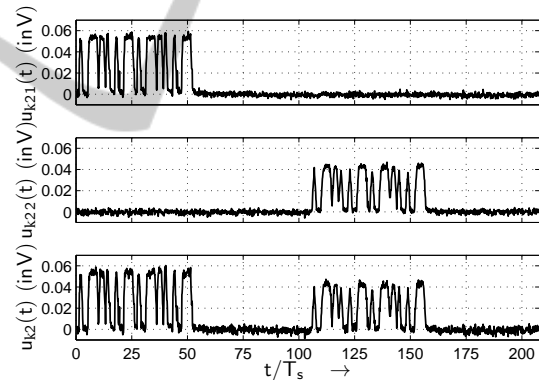


Figure 11: Measured received signal $u_{k2}(t)$ within the (2×2) MIMO system with respect to the pulse frequency $f_T = 1/T_s = 625$ MHz assuming a fibre length 1.9 km.

6 CONCLUSION

In this contribution a successful receiver design for a (2×2) optical MIMO system was presented. The receiver consisting of the following components: frame synchronisation, symbol clock recovery, channel estimator and equalizer was applied to a 1.9 km MIMO testbed. The successful implementation of the MIMO receiver was demonstrated by the open eye-diagram.

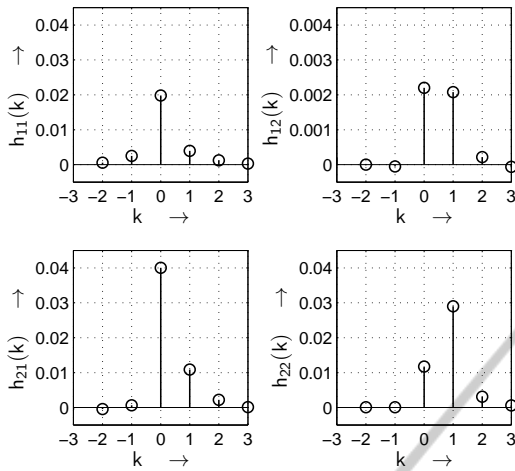


Figure 12: Estimated channel coefficients of the measured (2×2) MIMO signal assuming a pulse frequency of $f_T = 1/T_s = 625$ MHz and a fibre length 1.9 km .

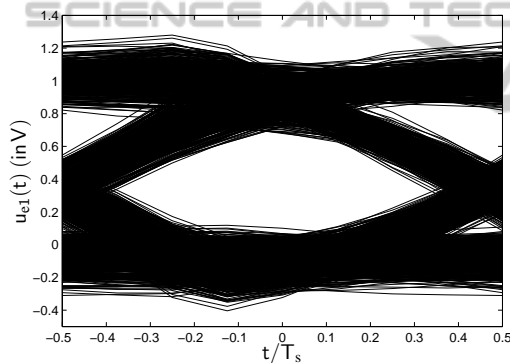


Figure 13: Eye-diagram of received signal $u_{e1}(t)$ after equalization.

ACKNOWLEDGEMENTS

This work has been funded by the German Ministry of Education and Research (No. 03FH016PX3).

REFERENCES

- Ahrens, A. and Lochmann, S. (2013). Optical Couplers in Multimode MIMO Transmission Systems: Measurement Results and Performance Analysis. In *International Conference on Optical Communication Systems (OPTICS)*, pages 398–403, Reykjavik (Iceland).
- Amphawan, A. and Al Samman, N. M. A. (2013). Tiering Effect of Solid-Core Photonic Crystal Fiber on controlled Coupling into Multimode Fiber. In *Photonic Fiber and Crystal Devices: Advances in Materials*

and Innovations in Device Applications (SPIE 8847), pages 88470Y–88470Y–6.

- Bingham, J. A. C. (1988). *The Theory and Practice of Modem Design*. Wiley, New York.
- Franz, B. and Blow, H. (2012). Experimental Evaluation of Principal Mode Groups as High-Speed Transmission Channels in Spatial Multiplex Systems. *IEEE Photonics Technology Letters*, 24:1363–1365.
- Giles, I., Obeysekera, A., C., R., Giles, D., Poletti, F., and Richardson, D. (2012). All Fiber Components for Multimode SDM Systems. In *IEEE Summer Topical 2012: Space Division Multiplexing for optical Systems and Networks*, pages 212–213.
- Gu, R., IP, E., Li, M. J., Huang, Y. K., and Kahn, J. M. (2013). Experimental Demonstration of a Spatial Light Modulator Few-Mode Fiber Switch for Space-Division Multiplexing. In *Frontiers in Optics*.
- Kühn, V. (2006). *Wireless Communications over MIMO Channels – Applications to CDMA and Multiple Antenna Systems*. Wiley, Chichester.
- Richardson, D. J., Fini, J., and Nelson, L. (2013). Space Division Multiplexing in Optical Fibres. *Nature Photonics*, 7:354–362.
- Sandmann, A., Ahrens, A., and Lochmann, S. (2014a). Equalisation of Measured Optical MIMO Channels. In *International Conference on Optical Communication Systems (OPTICS)*, Vienna (Austria).
- Sandmann, A., Ahrens, A., and Lochmann, S. (2014b). Experimental Description of Multimode MIMO Channels utilizing Optical Couplers. In *15. ITG-Fachtagung Photonische Netze*, Leipzig (Germany).
- Singer, A. C., Shanbhag, N. R., and Bae, H.-M. (2008). Electronic Dispersion Compensation– An Overview of Optical Communications Systems. *IEEE Signal Processing Magazine*, 25(6):110–130.
- Tse, D. and Viswanath, P. (2005). *Fundamentals of Wireless Communication*. Cambridge, New York.
- van Etten, W. (1975). An Optimum Linear Receiver for Multiple Channel Digital Transmission Systems. *IEEE Transactions on Communications*, 23(8):828–834.
- van Etten, W. (1976). Maximum Likelihood Receiver for Multiple Channel Transmission Systems. *IEEE Transactions on Communications*, 24(2):276–283.
- Winzer, P. (2012). Optical Networking beyond WDM. *IEEE Photonics Journal*, 4:647–651.